

# High-transparency Ni/Au bilayer contacts to n-type GaN

Abhishek Motayed

*Department of Electrical Engineering, Howard University, 2300 Sixth Street NW, Washington, DC 20059*

Albert V. Davydov and Leonid A. Bendersky

*Metallurgy Division, National Institute of Standards and Technology, 100 Bureau Drive, Mail Stop 8555, Gaithersburg, Maryland 20899-8555*

Mark C. Wood and Michael A. Derenge

*U.S. Army Research Laboratory, Mail Stop AMSRL-SE-RL, 2800 Powder Mill Road, Adelphi, Maryland 20783-1138*

Dong Feng Wang

*Department of Electrical Engineering, Howard University, 2300 Sixth Street NW, Washington, DC 20059*

Kenneth A. Jones

*U.S. Army Research Laboratory, Mail Stop AMSRL-SE-RL, 2800 Powder Mill Road, Adelphi, Maryland 20783-1138*

S. Noor Mohammad<sup>a)</sup>

*Department of Electrical Engineering, Howard University, 2300 Sixth Street NW, Washington, DC 20059*

(Received 25 March 2002; accepted 26 July 2002)

A unique metallization scheme has been developed for obtaining both Schottky and low-resistance Ohmic contacts to *n*-GaN. It has been demonstrated that the same metallization can be used to make both Schottky and Ohmic contacts to *n*-GaN using a Ni/Au bilayer composite with Ni in contact to GaN. Using this metallization, contacts with a specific contact resistivity,  $\rho_s$ , as low as  $6.9 \times 10^{-6} \Omega \text{ cm}^2$  for a doping level of  $5.0 \times 10^{17} \text{ cm}^{-3}$  was obtained after annealing the sample for 10 s at 800 °C in a rapid thermal annealer. The presence of only (111)Au and (111)Ni peaks in the x-ray diffraction (XRD) pattern of as-deposited samples indicates that both metals participate to form epitaxial or highly textured layers on the basal GaN plane. When the contact layer is annealed, Au and Ni react with GaN creating interfacial phases. Both XRD and transmission electron microscopy confirm that  $\text{Ni}_3\text{Ga}$  and  $\text{Ni}_2\text{Ga}_3$  intermetallic phases together with Au and Ni based face-centered-cubic solid solutions, are formed during annealing. The high optical transmission achieved (in the range of 400–700 nm) through this contact after annealing suggests that it is, indeed, very useful for electro-optic device applications. The contacts also demonstrate exceptional thermal stability. Experimental data suggest that the formation of interfacial phases with a low work function is responsible for the low contact resistance of the system. The Ni–Au layer forms a robust composite enabling the contacts to have high-temperature applications. Unlike the Ni/Au Ohmic contact, the Ni/Au Schottky contact to *n*-GaN has a relatively large barrier height. Improved material quality and Schottky contact technology are needed to improve upon the reverse breakdown voltage. © 2002 American Institute of Physics. [DOI: 10.1063/1.1509109]

## I. INTRODUCTION

The last several years have seen rapid developments in the creation of optical devices, such as laser diodes and optical detectors, made from the group III nitride semiconductors.<sup>1,2</sup> Ohmic and Schottky contacts are crucial for the success of these devices. A number of metals such as Au, Ni, Ti, Pd, Pt, PtSi, Ni/Au, Pt/Au, Cr/Al, Ti/Al/Ni/Au, and Cr/Al/Ni/Au have been deposited on nitride materials for this purpose, and the electrical characteristics of these contacts have been investigated.<sup>3–7</sup>

Highly transparent contacts are important for many optoelectronic devices including lasers, light-emitting diodes, and optoelectronic field-effect transistors (FETs). For opto-

electronic FETs with light incident from the top surface, both *n*-type Ohmic and Schottky contacts should be transparent.<sup>8–10</sup> A low-resistance *p*-electrode, low-resistance *n*-electrode, and high-barrier-height Schottky contact made from a highly transparent metal or metal combination is an important issue for the fabrication of GaN-based optical emitters and detectors. In the past, well-known transparent conducting films such as indium tin oxide (ITO) and cadmium tin oxide (CTO) have found wide use as electrodes for light-emitting diodes.<sup>11,12</sup> An ITO transparent conducting film deposited on *n*-GaN (carrier concentration  $\sim 3 \times 10^{17} \text{ cm}^{-3}$ ) and *p*-GaN ( $\sim$ carrier concentration of  $3 \times 10^{17} \text{ cm}^{-3}$ ), and annealed appropriately, should produce a Schottky contact. The formation of an ITO Ohmic contact on GaN should be possible if the carrier concentration of GaN

<sup>a)</sup> Author to whom correspondence should be addressed; electronic mail: snm@msrce.howard.edu

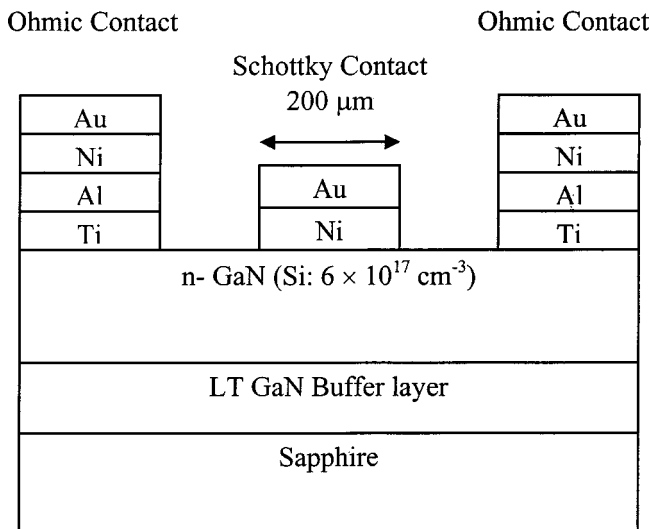


FIG. 1. Schematic structures of metallization used for the Schottky Ni/Au (500 Å/250 Å) contact on GaN with Ohmic metallization of the Ti/Al/Ni/Au (300 Å/1000 Å/300 Å/250 Å) multiplayer contact on *n*-GaN.

exceeds  $\sim 1 \times 10^{18} \text{ cm}^{-3}$ . For some optical devices very high doping ( $> 1 \times 10^{18} \text{ cm}^{-3}$ ) may not be possible, and even if it is possible, it may not be desirable, suggesting that it is important to find means to fabricate a low-resistance Ohmic contact onto moderately doped material. For GaN, a hole concentration higher than  $10^{18} \text{ cm}^{-3}$  is difficult to accomplish even by increasing the Mg or Be dopant density to as high as  $10^{20} \text{ cm}^{-3}$ . Ni/Au deposited on GaN after alloying forms a highly transparent layer. To utilize one single metal or bilayer, such as a Ni/Au bilayer, for a Schottky contact and a transparent Ohmic contact to *n*- and *p*-type GaN would be beneficial for the fabrication of optical devices. Both Ni- and Au-based Ohmic contacts to *p*-type GaN have recently been successful.<sup>13,14</sup> A Ni/Au bilayer can also be very useful<sup>15–20</sup> to fabricate an Ohmic contact to *p*-type GaN.

Our objective in the present investigation is to develop a metallization scheme that allows the same metallization to fabricate both Schottky and Ohmic contacts to *n*-GaN, and to explore the fundamental physics underlying these Schottky and the low-resistance Ohmic contacts.

## II. EXPERIMENTAL PROCEDURE

The GaN films for this study were grown by the metal organic chemical vapor deposition (MOCVD) method on (0001) sapphire substrates that were  $\sim 400 \mu\text{m}$  thick. Prior to growth, the substrate was cleaned by heating in a hydrogen atmosphere in the MOCVD chamber up to  $1100^\circ\text{C}$ . An undoped low-temperature 30-nm-thick GaN buffer layer was then deposited on it. Finally, 1- $\mu\text{m}$ -thick GaN epilayer doped with silicon by a 10 sccm flow of silane was grown on the top of the GaN buffer layer.

For characterizing the NiAu Schottky contact, Al/Ti/Ni/Au Ohmic contacts were made to GaN, as shown in Fig. 1. Prior to the processing of the samples, they were cleaned using the standard procedure that involves a 3 min heated

ultrasonic bath successively in trichloroethylene, acetone, and finally, methanol. The samples were then dipped in a heated bath of  $\text{NH}_4\text{OH}:\text{H}_2\text{O}_2:\text{H}_2\text{O}$  (1:1:5) for 3 min, followed by a 3 min dip in a heated  $\text{HCl}:\text{H}_2\text{O}_2:\text{H}_2\text{O}$  (1:1:5) mixture. After photolithography, the samples were dipped into  $\text{HF}:\text{HCl}:\text{H}_2\text{O}$  (1:1:10) for 15 s, and finally, rinsed in  $\text{H}_2\text{O}$ , and dried just before the metals were deposited. Except for Au, the metals were deposited by electron-beam evaporation; the Au was evaporated thermally. During evaporation and metallization, the base pressure of the vacuum chamber was maintained at about  $10^{-7}$  Torr. For the Schottky contact, the thickness of the Ohmic electrode (Ti/Al/Ni/Au) was (300 Å/1000 Å/300 Å/300 Å), which was annealed following the procedure of Fan *et al.*<sup>21</sup> Graphite crucibles were used to evaporate 500 Å of Ni and 250 Å of Au, both 99.999% pure, on the patterned samples. The substrates were kept at room temperature during the evaporation. Following the metallization, the photoresist lift-off was performed in acetone to pattern the metals. The fabrication process yielded an array of 200- $\mu\text{m}$ -diam circular dots, inside a 300- $\mu\text{m}$ -diam opening of field Ohmic contacts. The area of the opening of the field contact was 2.25 times that of the inner Schottky dot.

To investigate the performance of the Ni/Au Schottky diodes, capacitance–voltage (*C–V*) measurements were made using a computer-interfaced HP 4912-A LF impedance analyzer meter connected to a probe station. It was operating at 100 kHz. A plot of reverse capacitance of the depletion region of the Ni/Au Schottky contacts on GaN was then performed as a function of reverse voltage. The purpose of this measurement to determine the nature of the depletion region. In the absence of an oxide layer between the metal and the semiconductor, the capacitance of a Schottky diode varies with applied gate bias as

$$C^{-2} = a_T - b_T V, \quad (1)$$

where  $a_T$  and  $b_T$  are constants

$$a_T = \frac{2(aV_{bi} - k_B T)}{q^2 \epsilon_s N_d}, \quad (2)$$

and

$$b_T = \frac{2}{q \epsilon_s N_d}, \quad (3)$$

where  $q$  is the electronic charge,  $k_B$  is the Boltzmann constant,  $T$  is the absolute temperature,  $\epsilon_s$  is the dielectric constant, and  $N_d$  is the doping concentration of the GaN sample. While  $V$  is the applied bias,  $V_{bi}$  is the built-in potential given by

$$V_{bi} = \phi_B / q - V_n, \quad (4)$$

with

$$V_n = \frac{k_B T}{q} \ln \left( \frac{N_c}{N_d} \right). \quad (5)$$

$N_c$  is the effective density of states for electrons in the conduction band.

Mesa structures for transmission line method (TLM) measurements for the Ohmic contacts were created by reac-

tive ion etching (RIE) of the GaN epilayer. A Plasma-Therm 790 series chamber was employed for this purpose. The RIE was accomplished by flowing  $\text{Cl}_2$  gas at 15 sccm for 4 min. The operating pressure was 10 mTorr, and the power was 150 W. The mesas were patterned, and a number of Ni/Au bilayers of several different thicknesses were deposited. While Ni was evaporated by an electron-beam evaporator, Au was evaporated thermally. The TLM structure thus created by the lift-off process had 11 rectangular contact pads of  $300 \times 300 \mu\text{m}^2$  dimension. The spacings between them were 2, 5, 10, 15, 20, 30, 40, 50, 60, and  $90 \mu\text{m}$ , respectively. A rapid thermal anneal of the samples was then performed in argon gas at various temperatures, and for different time intervals. Current–voltage ( $I$ – $V$ ) characteristics of various contact layers were measured before and after the thermal annealing, and the TLM measurements were performed for those contacts that had linear  $I$ – $V$  characteristics.

X-ray diffraction (XRD) measurements were carried out to determine the possible reaction mechanisms by identifying new phases created by the anneals. X-ray diffraction data were collected using a Phillips diffractometer equipped with incident soler slits, theta-compensating slits, a 0.2 mm receiving slit, a graphite monochromator, and a scintillation detector. Data were collected at ambient temperatures using Cu  $K\alpha$  radiation with a  $0.02^\circ$   $2\theta$  step size, and a 3 s count time. The observed  $2\theta$  peak positions were corrected using Standard Reference Material 660, and a  $\text{LaB}_6$  compound as an external calibrant. A Phillips 430 transmission electron microscope (TEM) operated at 300 keV and equipped with an energy dispersive x-ray spectrometer (EDS) was employed to obtain structural and compositional information at the metal/semiconductor interface.

### III. RESULTS AND DISCUSSIONS

#### A. Current–voltage characteristics of Schottky contacts

The current–voltage characteristics of the Ni/Au Schottky contacts are shown in Fig. 2. The current is given by the conventional equation

$$I = I_0 \exp\left(\frac{qV}{nk_B T}\right) \left[ 1 - \exp\left(-\frac{qV}{k_B T}\right) \right], \quad (6)$$

where  $I_0$  is the saturation current,  $V$  is the applied bias, and  $n$  is the ideality factor. The Schottky barrier diodes were subjected to several different thermal treatments. It is apparent from the  $I$ – $V$  characteristics in Fig. 2 that annealing led to a decrease of the Schottky barrier height. The  $I$ – $V$  characteristics of the *as-deposited* contact showed both forward and reverse barriers at the metal–semiconductor interface. From the simple band diagram of the metal– $n$ -type semiconductor junction, it is apparent that when the junction is forward biased electrons from the semiconductor overcome the forward barriers, which is the built-in potential  $V_{\text{bi}}$  in order to flow into the metal. In reverse bias, on the other hand, electrons following from the metal to the semiconductor overcome a barrier height, which under low carrier tunneling condition, is the Schottky barrier height of that particular metal semiconductor system. Also, the  $I$ – $V$  characteristics of

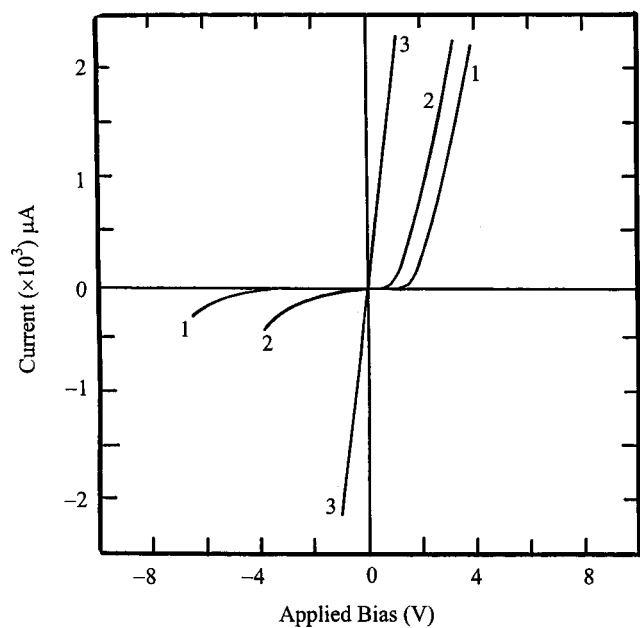


FIG. 2. Room-temperature current–voltage characteristics of Ni/Au ( $500 \text{ \AA}/250 \text{ \AA}$ ) Schottky diodes to  $n$ -GaN (doping density  $N_d = 6.0 \times 10^{17} \text{ cm}^{-3}$ ). The Ohmic contact for these diodes was an Al/Ti/Ni/Au ( $300 \text{ \AA}/1000 \text{ \AA}/300 \text{ \AA}/250 \text{ \AA}$ ) multilayer contact. Curve 1 corresponds to Ni/Au Schottky contacts without heat treatment, curve 2 to Ni/Au Schottky contacts annealed at  $600^\circ\text{C}$  for 20 s, and curve 3 to Ni/Au Schottky contacts annealed at  $750^\circ\text{C}$  for 20 s.

the *as-deposited* Ni/Au Schottky barrier diodes showed a reverse breakdown voltage of  $\sim 4$  V. Interestingly, this is lower than that obtained by other groups, due probably to an enhanced tunneling component in reverse saturation current, and the reduction in the effective barrier height resulting from the image-charge lowering because of the higher doping concentration of our samples. The  $I$ – $V$  characteristics of the diodes annealed at  $600^\circ\text{C}$  for 20 s revealed that after annealing the forward conduction started at a lower voltage and that the reverse breakdown voltage has been reduced from 4 to 1.6 V. This indicated possible reactions between Ni and GaN taking place at the interface, and leading to the reduction in the Schottky barrier height. Lowering of the built-in potential consequently followed. Annealing of the diode structures at  $750^\circ\text{C}$  for 20 s caused the  $I$ – $V$  characteristics to be perfectly linear. One may thus argue that reactions between the Ni and GaN interface at this temperature due to thermal annealing were efficient enough to change the Ni Schottky contacts into Ni Ohmic contacts.

#### B. Capacitance–voltage ( $C$ – $V$ ) characteristics of Schottky contacts

Capacitance–voltage measurement is an important tool to better determine the characteristics of metal–semiconductor contacts. The room-temperature variations of the absolute values of  $C$  and  $C^{-2}$  obtained as functions of applied reverse voltage  $V$  at a frequency of 100 kHz are shown in Fig. 3. From Fig. 3 it is apparent that the  $C^{-2}$  vs  $V$  plot exhibited a linear nature as predicted by Eq. (1), and that  $C^{-2}$  decreased with increasing reverse bias  $V$ . The tangent to the  $C^{-2}$  vs  $V$  plot emerged essentially from a point in the

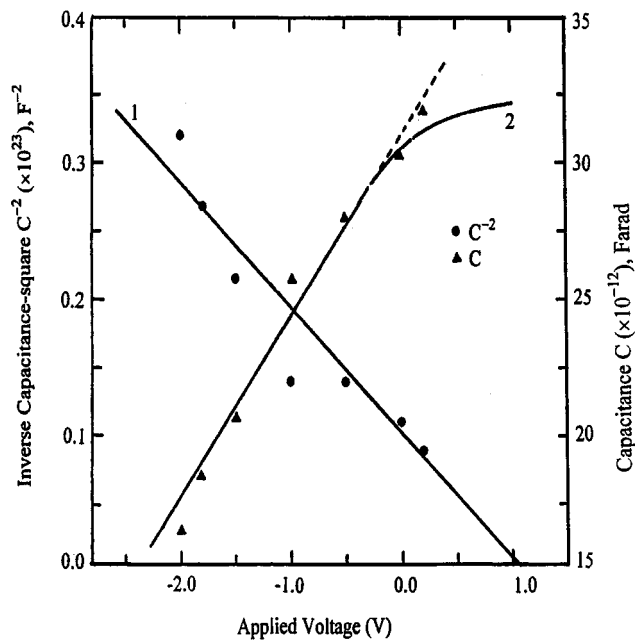


FIG. 3. Room-temperature variation of absolute capacitance  $C$  and the inverse capacitance square  $C^{-2}$  with applied bias in Ni/Au Schottky contacts to  $n$ -GaN (doping density  $N_d = 6.0 \times 10^{17} \text{ cm}^{-3}$ ). Curve 1 is the least-square fit for  $C$  and curve 2 is the least-square fit for  $C^{-2}$ . The small solid circles are experimental data for  $C^{-2}$ , and small solid triangles are experimental data for  $C$ , respectively.

voltage axis. The  $C$  vs  $V$  plot showed that capacitance  $C$  decreases less slowly with increasing applied bias, because deep-level traps were increasingly exposed by the increase in the depletion region width caused by the reverse bias. These traps emitted electrons. In order to determine the doping density of the GaN sample, we carried out numerical calculations using Eqs. (1)–(3), and the dielectric constant  $\epsilon_s = 9.0$ . Capacitance per unit area of the diode was used in the respective equations for the calculation. The calculations yielded  $N_d = 5 \times 10^{17} \text{ cm}^{-3}$ , which is in close correspondence with  $N_d = 6 \times 10^{17} \text{ cm}^{-3}$  obtained from Hall measurements. A barrier height of 1.2 eV was obtained for the Ni/Au Schottky contact using Eqs. (4) and (5), and assuming that the effective density of states for electrons in the conduction band was  $N_c = 2.6 \times 10^{18} \text{ cm}^{-3}$ . Had the defect levels present in the system been appreciably large, all donor levels above the Fermi level would have been ionized by the applied bias. This would give a higher doping level near the interface. If the deep levels would follow an ac signal, usually at low frequencies, there would also be an additional contribution to the capacitance, which would result in an increase in the doping density  $N_d$  and a decrease in the slope of the  $C^{-2}$  vs  $V$  plot. Since the slope of the  $C^{-2}$  vs  $V$  plot of Fig. 3 remained nearly identical at various measurement frequencies, it is reasonable to assume that the presence of the deep levels insignificantly impacted the observed  $C^{-2}$  vs  $V$  characteristics of the diodes.

### C. Current–voltage characteristics of Ohmic contacts

Figure 4 shows the  $I$ – $V$  characteristics of the Ohmic contacts to  $n$ -GaN before and after annealing. As is apparent

from Fig. 4, the  $I$ – $V$  curves for the nonalloyed contact were nonlinear, but they became linear upon annealing. Measured specific contact resistances of the Ni/Au contacts to  $n$ -GaN as a function of metal thickness, alloying temperature, and alloying time are presented in Table I. It can be noted from Table I that the contacts became linear only after annealing at 800 °C. The contact resistances were obtained by the TLM measurements employing the measured sheet resistances as a function of gap spacing. Room-temperature resistance  $R_T$  between the two contacts was obtained by using a four-point-probe arrangement. The variation of total resistance with the spacing between the contacts is shown in Fig. 5. Specific contact resistance  $\rho_s$  was determined from a least-squares fit of the data, and, as expected,  $\rho_s$  for the annealed material was substantially lower than that for the unannealed material.

The sample, with Ni/Au bilayer thicknesses of 500 and 250 Å, and annealed at 800 °C for 5 s, yielded a specific contact resistance  $\rho_s = 1.3 \times 10^{-3} \Omega \text{ cm}^2$ , while the sample with same bilayer thickness annealed at 800 °C for 10 s showed quite a significant improvement in specific contact resistance ( $\rho_s = 1.4 \times 10^{-4} \Omega \text{ cm}^2$ ). However, annealing at the higher temperature of 850 °C proved to be detrimental in that the  $I$ – $V$  characteristics now became nonlinear. The nonlinear  $I$ – $V$  characteristics of these contacts obtained after annealing at 850 °C resulted probably because of interface degradation due to extensive reaction of metals with GaN at the elevated temperature.

The surface morphology of the annealed contacts, as seen from scanning electron microscopy (SEM) and optical micrographs, is depicted in Fig. 6. It is noted that annealing at a temperature higher than 850 °C produces a high concentration of pits in the metal film. As a result, the film appeared to be porous with island-like formations on the surface. It is also observed that the thickness of the Ni (which is in intimate contact with GaN) had a profound effect on the electrical performance of the contacts. Three different thicknesses of the Ni layer, and the effect of these thicknesses on contact performance, were investigated as a function of annealing temperature. It was revealed (see Table I) that increasing the thickness of the Ni layer above 500 Å increased the contact resistivity. A similar trend was also observed when the thickness of Ni was decreased: contacts with 150-Å-thick Ni and 250-Å-thick Au failed to show Ohmic behavior even after annealing at 800 °C. Thus, it is evident that a thickness of 500 Å for Ni was quite optimum for obtaining a low-resistance Ohmic contact to  $n$ -type GaN at an annealing temperature of 800 °C. Increasing the thickness of the top Au layer (by 100 Å, from 250 to 350 Å) resulted in a striking improvement in the specific contact resistance. The lowest specific contact resistance in the range of  $6.9 \times 10^{-6} \Omega \text{ cm}^2$  was obtained with a Ni/Au contact layer, 500 Å/350 Å thick, after annealing at 800 °C for 10 s.

### D. Optical transmission

During the last several years a number of attempts have been made for using the Ni/Au metallization to accomplish highly transparent Ohmic contacts to  $p$ -GaN. Sheu *et al.*<sup>15</sup>

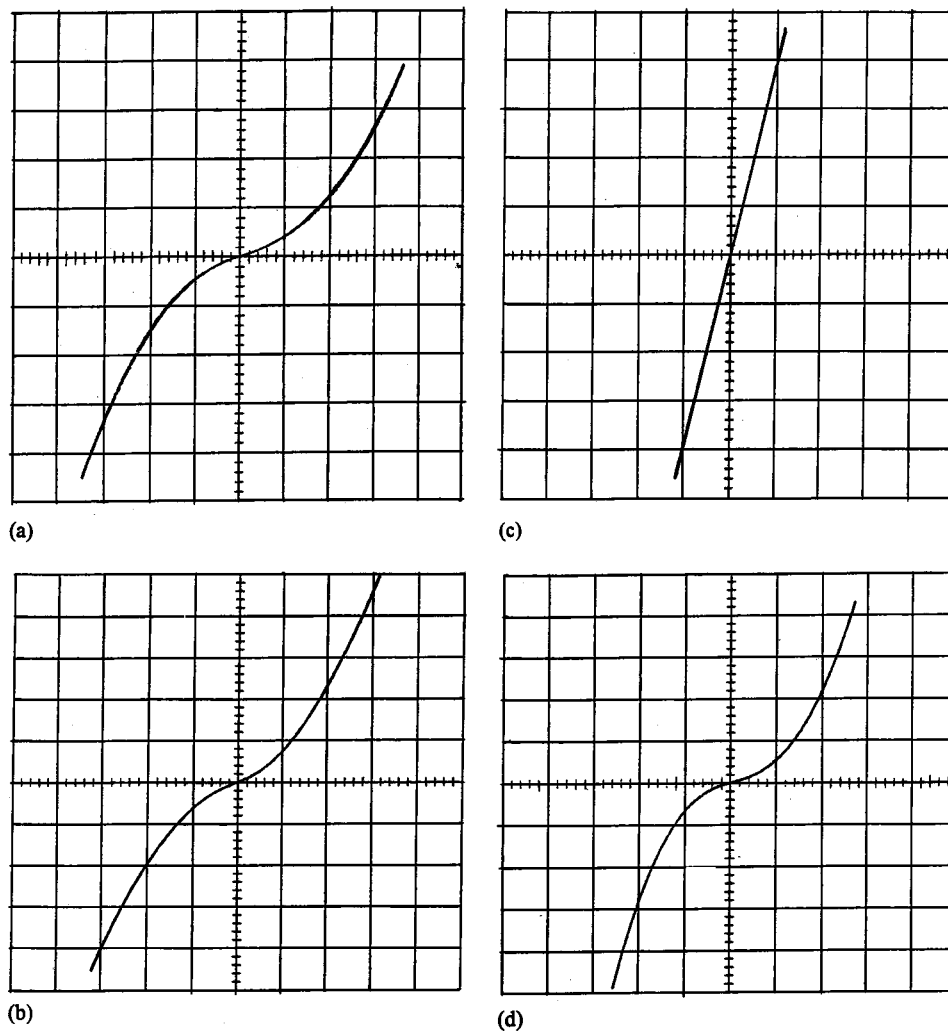


FIG. 4. Room-temperature current-voltage characteristics of the Ni/Au (500 Å/250 Å) Ohmic contact to *n*-GaN samples of doping density  $6.0 \times 10^{17} \text{ cm}^{-3}$ : (a) *as deposited* (each small division in the vertical scale is for 200  $\mu\text{A}$  and each small division in the horizontal scale is for 1 V); (b) annealed at 600 °C for 10 s (each small division in the vertical scale is for 200  $\mu\text{A}$  and each small division in the horizontal scale is for 1 V); (c) annealed at 800 °C for 10 s (each small division in the vertical scale is for 1 mA and each small division in the horizontal scale is for 500 mV); and (d) annealed at 850 °C for 10 s (each small division in the vertical scale is for 200  $\mu\text{A}$  and each small division in the horizontal scale is for 1 V).

observed that a Ni/Au (20 Å/60 Å) contact to *p*-GaN, annealed at 500 °C in an  $\text{N}_2$  ambient, can exhibit a light transmittance of 88% (at a wavelength  $\lambda=470 \text{ nm}$ ), and still can have a contact resistivity of  $2.43 \times 10^{-2} \Omega \text{ cm}^2$ . Ho *et al.*<sup>16</sup> selected, on the other hand, a Ni/Au (100 Å/50 Å) contact to *p*-GaN annealed at 400 °C for 10 min in air, and observed

that the light transmittance of the contact is about 70% (at  $\lambda=470 \text{ nm}$ ), and the specific contact resistance is  $1.00 \times 10^{-4} \Omega \text{ cm}^2$ . Recently, Jang, Park, and Seong<sup>20</sup> observed that a Ni/Au (150 Å/50 Å) contact to *p*-GaN annealed at 500 °C for 1 min in  $\text{N}_2$  exhibits a light transmittance of about 97% (at  $\lambda=470 \text{ nm}$ ), and a specific contact resistance of

TABLE I. Specific contact resistance of Ni/Au contacts to *n*-type GaN films as function of metal thicknesses, alloying temperatures, and alloying time.

Ni/Au contact thickness	Annealing temperature (°C)	Annealing time (s)	<i>I</i> - <i>V</i> characteristics	Specific contact resistance ( $\Omega \text{ cm}^2$ )
Ni(500 Å)/Au(250 Å)	<i>As deposited</i>	...	Nonlinear	...
Ni(500 Å)/Au(250 Å)	600	10	Nonlinear	...
Ni(500 Å)/Au(250 Å)	700	10	Nonlinear	...
Ni(500 Å)/Au(250 Å)	800	5	Linear	$1.3 \times 10^{-3}$
Ni(500 Å)/Au(250 Å)	800	10	Linear	$1.4 \times 10^{-4}$
Ni(500 Å)/Au(250 Å)	850	10	Nonlinear	...
Ni(500 Å)/Au(150 Å)	<i>As deposited</i>	...	Nonlinear	...
Ni(500 Å)/Au(150 Å)	800	10	Linear	$1.3 \times 10^{-4}$
Ni(500 Å)/Au(350 Å)	<i>As deposited</i>	...	Nonlinear	...
Ni(500 Å)/Au(250 Å)	800	10	Linear	$6.9 \times 10^{-6}$
Ni(150 Å)/Au(250 Å)	<i>As deposited</i>	...	Nonlinear	...
Ni(150 Å)/Au(250 Å)	800	10	Nonlinear	...
Ni(650 Å)/Au(250 Å)	<i>As deposited</i>	...	Nonlinear	...
Ni(650 Å)/Au(250 Å)	800	10	Linear	$1.3 \times 10^{-4}$

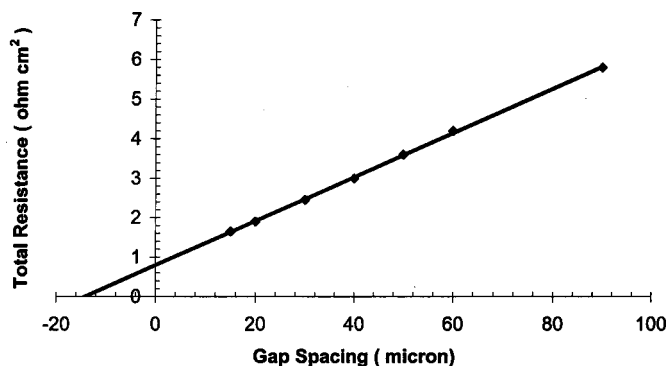


FIG. 5. Room-temperature variation of total resistance with contact spacing for the Ni/Au bilayer Ohmic contacts to *n*-GaN of doping density  $N_d = 6.0 \times 10^{17} \text{ cm}^{-3}$ . Small solid circles are the experimental data points. Solid lines represent the least-squares regression fit to the experimental data.

$2.5 \times 10^{-3} \Omega \text{ cm}^2$ . No light transmittance study of the Ni/Au contact to *n*-GaN seems to have been reported in the literature.

The optical transmission through our Ni/Au contact to *n*-GaN was studied using a Shimadzu UV-3101PC scanning spectrometer. The results are presented in Fig. 7. Figure 7 shows the light transmission (%) spectra as a function of

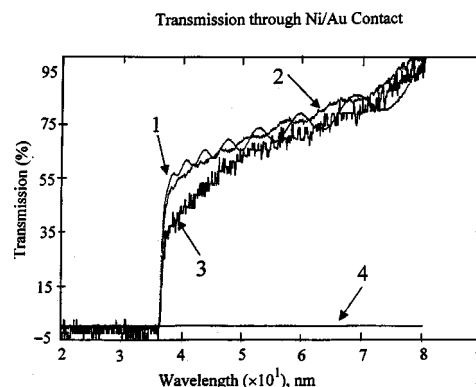


FIG. 7. Transmission characteristics of the Ni/Au (500 Å/250 Å) bilayer before and after annealing at different temperatures. Curve 1 corresponds to the GaN film, curve 2 to GaN with the Ni/Au film annealed at 850 °C, curve 3 to GaN with the Ni/Au film annealed at 800 °C, and curve 4 to GaN with the Ni/Au as-deposited film.

wavelength  $\lambda$  of light for GaN film, GaN with Ni/Au *as-deposited* film, GaN with a Ni/Au film annealed at 800 °C, and a GaN with Ni/Au film annealed at 850 °C. For all contacts, the Ni/Au film had a thickness of (500 Å/250 Å). Figure 7 indicates that high optical transmission can indeed be achieved through annealed Ni/Au contacts, although there is a tradeoff between the contact resistance and light transmittance. Light transmission as high as 88% (at  $\lambda = 470 \text{ nm}$ ) was achieved through a Ni/Au contact, which was annealed at 800 °C for 10 s, and had a specific contact resistance of  $1.4 \times 10^{-4} \Omega \text{ cm}^2$ . At the higher annealing temperature of 850 °C, 94% light transmittance was obtained, but the contact had nonlinear *I*-*V* characteristics, implying that it was rather Schottky in nature. The transmission (%) was essentially zero for an optical wavelength  $\lambda$  lower than about 250 nm, and that it increased with increasing wavelength of the light for  $\lambda \geq 350 \text{ nm}$ , owing probably to the band-edge absorption of the underlying GaN film. A comparison of the performance of various contacts demonstrates that our contacts were far thicker than the contacts made on *p*-GaN. Yet, the light transmittance through our contact was quite high.

The increase in light transmission with increase in thermal alloying temperature of the contacts may plausibly be attributed to a gradual decrease in the Ni thickness due to a reaction with the GaN at increasing thermal alloying temperature. At the higher thermal alloying temperatures, Ni starts to form islands, thus creating voids in the metal film, which has been confirmed by TEM. This appears to be the cause of the transparency of the metal films. Based on these observations, it may be argued that the Ni/Au contact metalization can indeed be quite useful for optoelectronic device applications for which conducting transparent windows must be an essential element of the device structures. Transparent contacts assist in increasing the optical efficiency of those devices. Thus, depending on the thickness of the Ni/Au, an optimum thermal alloying temperature window would be needed to ensure a high transparency, and at the same time, good Ohmic contact resistivity of the contacts.

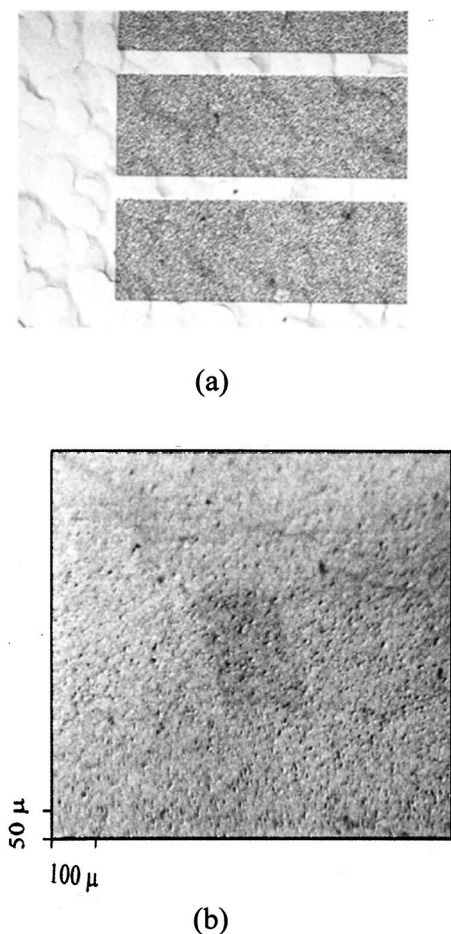


FIG. 6. (a) Optical micrograph of Ni/Au (500 Å/250 Å) contacts annealed at 800 °C for 10 s and (b) surface morphology of the films as seen in the SEM micrograph of the same contacts.

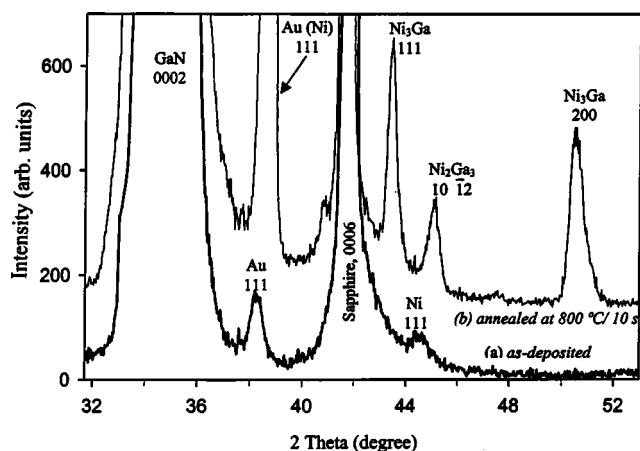


FIG. 8. XRD spectra of Ni/Au (500 Å/250 Å) contacts: (a) as deposited and (b) annealed at 800 °C for 10 s.

#### IV. MICROSTRUCTURAL CHARACTERIZATION

The primary contribution to the contact resistance was at the metal–semiconductor interface, where tunneling and thermionic field emission dominated the electron transport. A number of factors contributing to these effects tended to lower the contact resistance. Among them, narrowing of the tunneling barrier due to an increase in the doping level of the semiconductor was very important. In fact, this was the cause of the lower contact resistivity of the heavily doped samples.

##### A. X-ray diffraction analysis

As evident from Fig. 8(a), Au(111) and Ni(111) reflections were presented in the XRD pattern of the *as-deposited* Au/Ni/GaN/sapphire sample, suggesting that both metals formed highly textured layers on the basal GaN plane. The peak positions of both gold and nickel ( $38.20^\circ$  and  $44.51^\circ$   $2\theta$ , respectively), in the *as-deposited* samples, showed that there was no intermixing of the metals. Noticeably, the (111) peak intensity of Au was stronger than that of Ni in the *as-deposited* sample, suggesting that the degree of crystallinity of the Ni film was lower compared to that of the Au film of the *as-deposited* contact. As expected, the heat treatment at 800 °C for 10 s resulted in the formation of several different interfacial phases. The fcc solid solution of nickel in gold, Au(Ni), was identified by the shifted (111) reflection peak at the  $38.56^\circ$   $2\theta$  position in the annealed samples [see Fig. 8(b)]. The lattice parameter of the Au(Ni) solid solution, as calculated from the (111) reflection, equaled 4.046 Å, and corresponded to the  $\text{Au}_{1-x}\text{Ni}_x$  alloy composition of  $x = 0.06$ . This implies that 6 at. % of Ni was dissolved in Au. The calculation was made by applying Vegard's rule to the compositional dependence of the lattice parameter for the fcc Au-Ni solid solution. It was found that the intensity of the Au(Ni)(111) peak increased about 200 times as compared to the (111) peak of Au in the *as-deposited* sample. The intensity increase was a result of the larger volume fraction of the (111)-textured Au(Ni) solid solution phase. As will be discussed later, it was confirmed also by TEM. As a result of interfacial reactions, cubic  $\text{Ni}_3\text{Ga}$  [see Fig. 8(b)] with a (111) peak at  $43.30^\circ$   $2\theta$  and a (200) peak at  $50.45^\circ$   $2\theta$  positions,

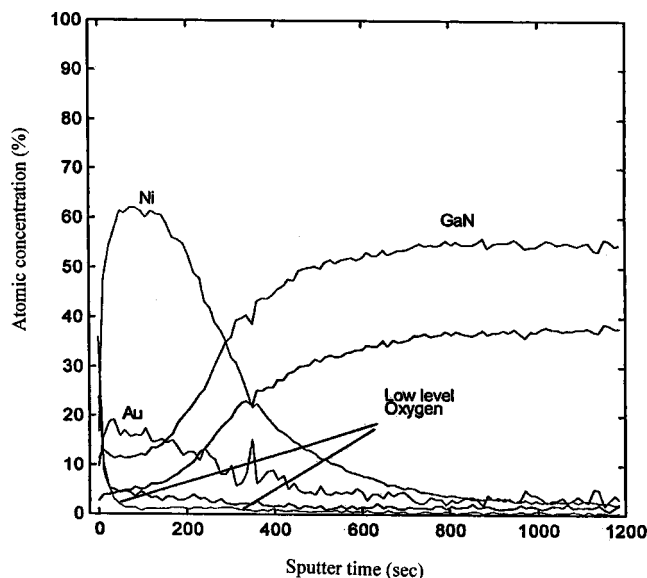


FIG. 9. Auger electron spectroscopy depth profiles of Ni/Au (500 Å/250 Å) contacts annealed at 800 °C for 10 s.

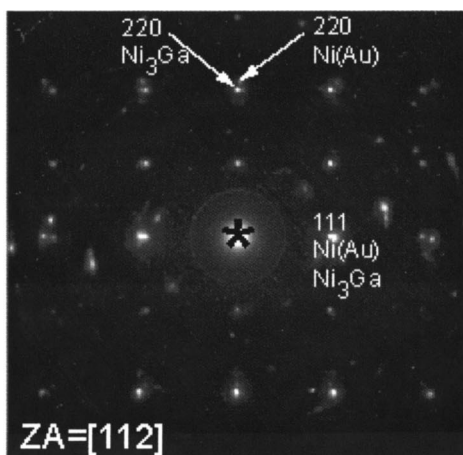
with a lattice parameter of 3.619 Å, was also identified. Further, the (10  $\bar{1}2$ ) reflection of hexagonal  $\text{Ni}_2\text{Ga}_3$  at the  $45.10^\circ$   $2\theta$  position was detected. The disappearance of the (111) Ni peak in the annealed sample was probably due to the Ni being consumed by the reactions with Ga or the masking effect of the  $\text{Ni}_3\text{Ga}$ (111) and  $\text{Ni}_2\text{Ga}_3$ (10  $\bar{1}2$ ) reflections.

##### B. Auger electron spectroscopic analysis

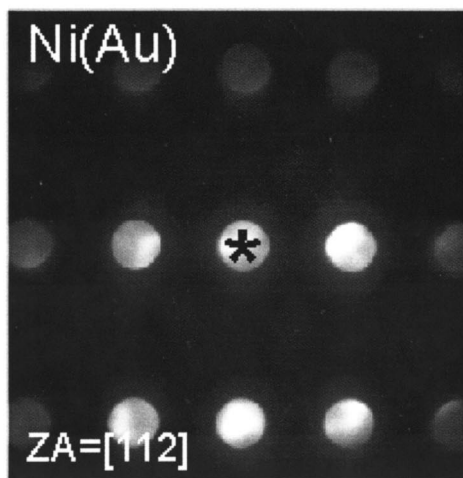
We found no evidence for interdiffusion between the metal layers and GaN of the preannealed contacts. The Auger electron spectroscopic (AES) depth profile of the annealed contact is shown in Fig. 9. Figure 9 reveals that there was a very low level of oxygen in the contacts. However, there was an increase in the oxygen content at the surface plausibly in the form of the oxide layer. This is an indication of the fact that annealing at very high temperature can actually lead to an increase in the resistivity of the contact. Due to annealing, Au diffused into the Ni layer and segregated at the metal/GaN interface. Consequently, some of the Ni appeared on the surface. There was also an extensive reaction between Ni and GaN. Possibly, as the reaction proceeded at high annealing temperature (800 °C), formation of the intermetallic compounds, viz.  $\text{Ni}_3\text{Ga}$  and  $\text{Ni}_2\text{Ga}_3$ , took place at the interface. During this time, nitrogen escaped from the microstructure via out-diffusion through the grain boundaries of the metal film.

##### C. Transmission electron microscopic analysis

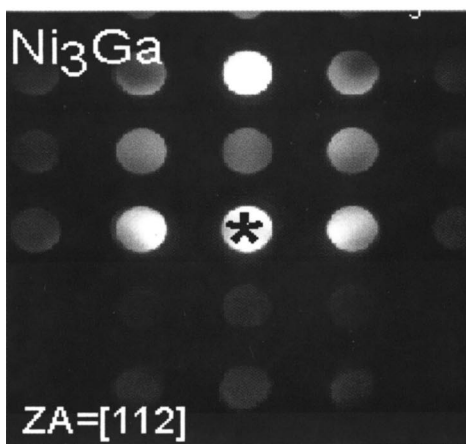
The TEM analysis of the sample annealed at 800 °C for 10 s demonstrated major changes in the morphology and the presence of several interfacial phases. Selected-area diffraction (SAD) patterns and an accompanying low magnification image of a cross-sectional specimen, are shown in Figs. 10 and 11(a)–11(c), respectively. According to the cross-sectional TEM, which is supported by the EDS analysis, there were grains with a fcc structure of solid solutions,



(a)



(b)



(c)

FIG. 10. Bright-field image of a cross-sectional TEM specimen of Au(250Å)/Ni(500Å) on GaN after annealing at 800 °C for 10 s in argon. Regions 1 and 2 are Au(Ni) and Ni(Au,Ga) fcc solid solutions, respectively. Note that Au diffused from the upper part of the metal film to the metal/GaN interface. The metal film structure changed from a continuous layer to an island-like morphology.

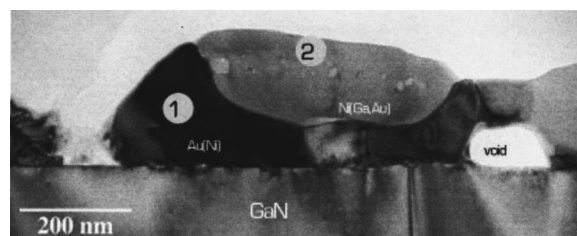


FIG. 11. Au/Ni/GaN/sapphire sample annealed at 800 °C for 10 s: (a) SAD pattern and (b) and (c) microdiffraction patterns from neighboring grains show the presence of fcc superlattice reflections as in (c), thus suggesting the coexistence of grains of the Ni-based solid solution and Ni<sub>3</sub>Ga phase.

Au(Ni) and Ni(Au,Ga) (see Fig. 11), as well as a fcc-based ordered Ni<sub>3</sub>Ga phase, in the film. However, the presence of binary or ternary nitrides at the interface was not detected during the TEM analysis. The identification of the highly textured Au-based solid solution and Ni<sub>3</sub>Ga phase in TEM and SAD is in line with the XRD results. The Au(Ni) alloy that was formed had the (111)∥(0001) orientation relationship at the basal GaN plane. This effectively “pushed out” the Ni-based phases from the interface toward the surface of the metal film. The morphology of the metal film was also significantly altered; the continuous layer adopted rather an island-like morphology after annealing (Fig. 11).

#### D. Discussions of overall microstructural analysis

As is evident from the TEM, AES, and XRD studies of the present microstructure, the reaction mechanism for Ohmic contact formation involved a number of important steps. Due to the thermal treatment, Ga out diffused from the crystal lattice reaction with Ni and forming Ni–Ga compounds. While Au diffused slowly through the Ni layer, effectively replacing the Ni layer, it also dissolved Ni in it forming a fcc phase of solid solution of Au(Ni). This type of layer reversal and formation of voids is typically observed for *p*-type GaN/Ni/Au contacts after annealing.<sup>22</sup> Because of high surface energy of the metals at the high annealing temperature, they formed island-like structures. Formation of the Au(Ni) alloy and intermetallic compounds, along with the modification of the GaN near-interface region, due to the thermal treatment, might be the possible cause of the low resistivity of the present contracts. This is one of the central results of the present investigation. It is strongly believed that the said intermetallic compounds, formed due to alloying, have actually a lower work function than that of Ni. This prediction is based on the reported<sup>23</sup> work function for Ni–Ba and Ni–Cs films, which are 2.6 and 1.65 eV, respectively. We believe that dissolving Ga in Ni, or forming an intermetallic phase, Ni<sub>3</sub>Ga, resulted in the creation of the low-work-function intermetallic compounds. The presence of these low-work-function intermetallic compounds near the GaN surface is actually responsible for reducing the barrier height of the metal–semiconductor interface. It is worth mentioning that several research groups<sup>24,25</sup> have claimed to detect the presence of Ni-nitride (e.g., NiN, Ni<sub>3</sub>N, Ni<sub>4</sub>N) phases at the interface due to heat treatment. However, remarkably, during the present microstructural analysis, no

such nitrides were observed in our TEM and XRD patterns. Increasing the thickness of the Au layer from 250 to 350 Å led to a dramatic decrease in the contact resistance after annealing. This was probably due to the fact that, after annealing, most of the Au diffused through the Ni layer in the sample with 250 Å of Au. In the samples with 350 Å of Au, there was a sufficient amount of Au still left on the top surface of the contact to provide a low resistance path for the current.

## V. THERMAL STABILITY ANALYSIS

The realization of a highly reliable low-resistance Ohmic contact is a major challenge to obtaining high-performance GaN-based devices. Particularly, high-power, high-temperature applications necessitate high thermal stability of metal/GaN contacts. Among various Ohmic contacts to GaN, Ti/Al-based contacts have emerged as the most convenient and widely used contacts to GaN. Yet, the Ti/Al system is such that it becomes highly resistive during annealing. The Al<sub>2</sub>O<sub>3</sub> coating formed on Al during annealing leads to an increase in contact resistance.

The present contacts were subjected to a thermal stress for 24 h at a temperature of 400 °C. Remarkably, for both contact structures, Ni/Au (500 Å/250 Å) and Ni/Au (500 Å/350 Å), there were no apparent indications of degradation of the *I*-*V* characteristics. The *I*-*V* characteristics of one of the contacts before and after thermal stressing is compared in Fig. 12(a). From Fig. 12 it is apparent that, for example, for an applied bias of 500 mV, while the current was 4 mA before thermal stress, it was about 3.75 mA after thermal stress. The curve was perfectly linear before and after annealing, implying that thermal stress caused only marginal degradation of the Ohmic characteristics of the contacts. The variations of the total resistance of the contacts as a function of contact pads, before and after thermal stress, are compared in Fig. 12(b). As is usually the case, these variations provided scattered points, which were then least-square fitted to yield a straight line. The various points obtained for the total resistance before and after thermal stress were scattered in such a manner that they hardly allowed two different least-square fits to be obtained for two different straight lines, one for resistances before thermal stress and the other for resistances after thermal stress. This implies that there was no apparent sign of the formation of a spiky interface and surface roughness due to thermal stress. The thermal stability of the present contacts is believed to arise from the fact that the intermetallic compounds formed due to alloying had a high melting point, and hence, high thermal stability.

## VI. CONCLUSION

In conclusion, it has been demonstrated that a low-resistance Ohmic contact can be made to *n*-GaN with a Ni/Au bilayer structure. Ni, with a work function of 5.1 eV, formed a Schottky contact when deposited on *n*-type GaN. The barrier height of the Ni/Au Schottky contacts to *n*-type GaN appeared to be significantly high. However, with the proper annealing temperature and time, the barrier height for Ni/Au films could be reduced owing to the formation of

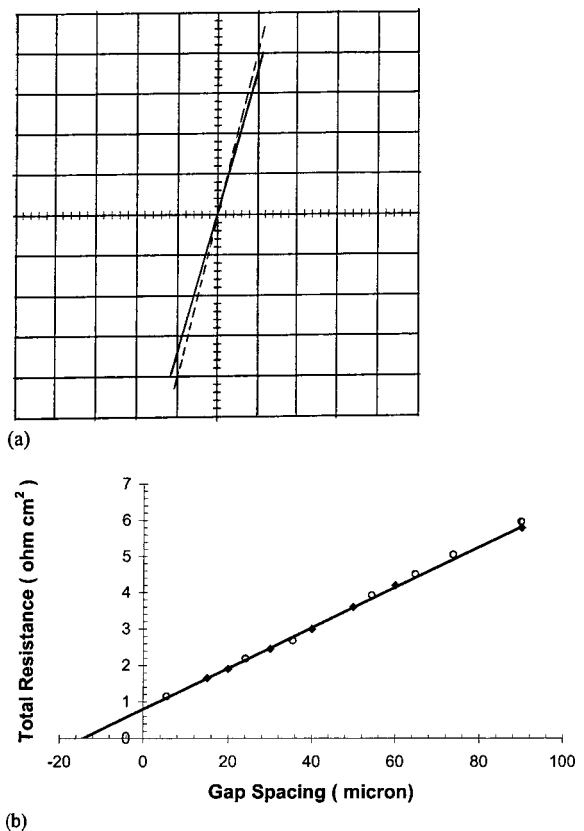


FIG. 12. Comparison of electrical characteristics of the Ni/Au (500 Å/250 Å) Ohmic contact to *n*-GaN doped with Si to  $6.0 \times 10^{17} \text{ cm}^{-3}$ . (a) Room-temperature current-voltage characteristics before and after the Ni/Au contacts (500 Å/250 Å) were thermally stressed at 400 °C for 24 h. The small solid squares represent the data for the prestressed condition, and the small open circles represent the data for the poststressed condition. Each small division in the vertical scale is for 1 mA and each small division in the horizontal scale is for 500 mV; (b) room-temperature variation of the total resistance with contact spacing for the Ni/Au (500 Å/350 Å) bilayer Ohmic contacts before thermal stressing (dashed line) and after thermal stressing (solid line) at 400 °C for 24 h.

interfacial alloys and compounds at the interface. XRD analysis demonstrated that *as-deposited* Ni/Au films have an epitaxial nature. Both XRD and TEM studies showed that Ni-Au solid solutions, together with intermetallic species, viz., Ni<sub>3</sub>Ga and Ni<sub>2</sub>Ga<sub>3</sub>, are formed in the vicinity of the interface. The contact resistivity was strongly dependent on the thickness of the Ni and Au layers, as well as on the annealing conditions. The specific contact resistance was about  $1.4 \times 10^{-4} \Omega \text{ cm}^2$  for 500-Å/250-Å-thick Ni/Au contacts after annealing at 800 °C for 10 s. However, specific contact resistance was in the range of  $6.9 \times 10^{-6} \Omega \text{ cm}^2$  for contacts with a 500-Å/350-Å-thick Ni/Au bilayer after annealing under identical conditions. A decrease in the thickness of Ni increased the contact resistance; thus, 150-Å-thick Ni contacts failed to show Ohmic characteristics even after annealing at 800 °C. It was thus concluded that a proper annealing temperature is very crucial for achieving low-resistance Ohmic contacts. Creating *N* vacancies by forming metal nitrides is generally considered to be a unique procedure to form low-resistance Ohmic contacts to *n*-type GaN. The present study established that low-resistance Ohmic contacts to *n*-type GaN can be achieved also by creating a highly

textured Au-based alloy at the interface, and by forming intergallium compounds with metals by heat treatment. Grati-fyingly, these contacts are also transparent; light transmittance through these contacts, as high as about 88% (at 470 nm), can easily be accomplished. Such a high transmittance is essential for devices useful for electro-optical applications.

The formation of the Ohmic contact involved the standard cleaning process of the *n*-GaN, which was followed by a dip in HF:HCl:H<sub>2</sub>O (1:1:10) solution before metal deposition. Except chemical treatments, no other means (for example, reactive ion etching of the surface) of removing the native oxide from GaN surface was employed. It is likely that the contact resistivity and the light transmission capability of the contacts would significantly improve if the *n*-GaN surface could be more efficiently cleaned before metallization.

### ACKNOWLEDGMENTS

The research is supported by the U.S. Army Research Laboratory, Adelphi, Maryland Grant No. DAAD17-00-C-0092. The authors appreciate illuminating discussions with Professor Changzhi Lu, Ousmane S. Diouf, James A. Griffin, Juan White, Crawford Taylor, and Dr. R. D. Vispute.

<sup>1</sup>For a review of issues germane to GaN-based devices, see S. N. Mohammad and H. Morkoç, *Prog. Quantum Electron.* **20**, 361 (1996).

<sup>2</sup>S. Nakamura and G. Fasol, *The Blue Laser Diode* (Springer, Heidelberg, 1997).

<sup>3</sup>T. G. Zhu, D. J. H. Lambert, B. S. Shelton, M. M. Wong, U. Chowdhury, and R. D. Dupuis, *Appl. Phys. Lett.* **77**, 2918 (2000).

<sup>4</sup>S. K. Noh and P. K. Bhattacharya, *Appl. Phys. Lett.* **78**, 3642 (2001).

<sup>5</sup>Q. J. Liu and S. S. Lau, *Solid-State Electron.* **42**, 677 (1998).

<sup>6</sup>A. C. Schmitz, A. T. Ping, M. Asif Khan, and I. Adesida, *Mater. Res. Soc. Symp. Proc.* **395**, 831 (1996).

<sup>7</sup>J. S. Foresi and T. D. Moustakas, *Appl. Phys. Lett.* **62**, 2859 (1993).

<sup>8</sup>A. A. De Salles and M. Murilo, *IEEE Trans. Microwave Theory Tech.* **MTT-39**, 2010 (1991).

<sup>9</sup>R. N. Simons, *IEEE Trans. Microwave Theory Tech.* **MTT-35**, 1444 (1987).

<sup>10</sup>M. Asif Khan, M. S. Shur, and Q. Chen, *Electron. Lett.* **31**, 2130 (1995).

<sup>11</sup>J. F. Lin, M. C. Wu, M. J. Jou, C. M. Chang, B. J. Lee, and Y. T. Tsai, *Electron. Lett.* **30**, 1793 (1994).

<sup>12</sup>M. Hagerott, J. Jeon, A. V. Nurmikko, W. Xie, D. C. Grillo, M. Kobayashi, and R. L. Gunshor, *Appl. Phys. Lett.* **60**, 2825 (1992).

<sup>13</sup>N. A. Papanicolaou, A. Edwards, Mulpuri V. Rao, J. Mittereder, and W. T. Anderson, *J. Appl. Phys.* **87**, 380 (2000).

<sup>14</sup>G. T. Dang, A. P. Zhang, M. M. Mishewa, F. Ren, J.-I. Chyi, C.-M. Lee, C. C. Chuo, G. C. Chi, J. Han, S. N. G. Chu, R. G. Wilson, X. A. Cao, and S. J. Pearton, *J. Vac. Sci. Technol. A* **18**, 1135 (2000).

<sup>15</sup>K. J. Sheu, Y. K. Su, G. C. Chi, P. L. Koh, M. J. Jou, C. M. Chang, C. C. Liu, and W. C. Hung, *Appl. Phys. Lett.* **74**, 2340 (1999).

<sup>16</sup>J.-K. Ho, C. S. Jong, C. C. Chiu, C. N. Huang, C. Y. Chen, and K. K. Shih, *L. C. Chen, F. R. Chen, and J. J. Kai J. Appl. Phys.* **86**, 4491 (1999); J. K. Ho, C. S. Jong, C. C. Chiu, C. N. Huang, C. Y. Chen, and K. K. Shih, *Appl. Phys. Lett.* **74**, 1275 (1999).

<sup>17</sup>L.-C. Chen, Fu-Rong Chen, J.-J. Chang, J. K. Ho, C. S. Jong, C. C. Chiu, C. N. Huang, C. Y. Chen, and K. K. Shih, *J. Appl. Phys.* **86**, 3826 (1999).

<sup>18</sup>J. K. Sheu, Y. K. Su, G. C. Chi, W. C. Chen, C. Y. Chen, C. N. Huang, J. M. Hong, Y. C. Yu, C. W. Wang, and E. K. Lin, *J. Appl. Phys.* **83**, 3172 (1998).

<sup>19</sup>Q. Qiao, L. S. Yu, S. S. Lau, J. Y. Lin, H. X. Jiang, and T. E. Haynes, *J. Appl. Phys.* **88**, 4196 (2000).

<sup>20</sup>J. S. Jang, S. J. Park, and T. Y. Seong, *J. Appl. Phys.* **88**, 5490 (2000).

<sup>21</sup>Z.-F. Fan, S. N. Mohammad, W. Kim, O. Aktas, A. E. Botchkarev, and H. Morkoç, *Appl. Phys. Lett.* **68**, 1672 (1996).

<sup>22</sup>L.-C. Chen, F.-R. Chen, J.-J. K. L. Chang, J.-K. Ho, C.-S. Jong, C. C. Chiu, C.-N. Huang, C.-Y. Chen, and K.-K. Shih, *J. Appl. Phys.* **86**, 3826 (1999).

<sup>23</sup>V. S. Fomenko, *Handbook of Thermionic Properties*, edited by G. V. Samsonov (Plenum, New York, 1966).

<sup>24</sup>D. Guo, F. M. Pan, M. S. Feng, R. J. Guo, P. F. Chou, and C. Y. Chang, *J. Appl. Phys.* **80**, 1623 (1996).

<sup>25</sup>J. K. Kim, J.-L. Lee, J. W. Lee, Y. J. Park, and T. Kim, *J. Vac. Sci. Technol. B* **17**, 2675 (1999).